JOURNAL OF MATERIALS SCIENCE: MATERIALS IN MEDICINE **16** (2005) 635–640

Microstructures and bond strengths of plasma-sprayed hydroxyapatite coatings on porous titanium substrates

IK-HYUN OH[1,*], N. NOMURA[2], A. CHIBA[2], Y. MURAYAMA[3], N. MASAHASHI[3], BYONG-TAEK LEE[4], S. HANADA[3]
[1]*Korea Institute of Industrial Technology (KITECH), P.O. Box #1, Wolgye-Dong, Gwangsan-gu, Gwangju, 506-824, South Korea*
E-mail: ihoh@kitech.re.kr
[2]*Department of Welfare Engineering, Iwate University, 4-3-5 Ueda, Morioka, 020-8551, Japan*
[3]*Institute for Materials Research (IMR), Tohoku University, 2-1-1 Katahira, Aoba-Ku, Sendai 980-8577, Japan*
[4]*School of Advanced Materials Engineering, Kongju National University, 182, Sinkwan-Dong, Kongju City, Chungnam, 314-701, South Korea*

Hydroxyapatite (HA) coating was carried out by plasma spraying on bulk Ti substrates and porous Ti substrates having a Young's modulus similar to that of human bone. The microstructures and bond strengths of HA coatings were investigated in this study. The HA coatings with thickness of 200–250 μm were free from cracks at interfaces between the coating and Ti substrates. XRD analysis revealed that the HA powder used for plasma spraying had a highly crystallized apatite structure, while the HA coating contained several phases other than HA. The bond strength between the HA coating and the Ti substrates evaluated by standard bonding test (ASTM C633-01) were strongly affected by the failure behavior of the HA coating. A mechanism to explain the failure is discussed in terms of surface roughness of the plasma-sprayed HA coatings on the bulk and porous Ti substrates.

1. Introduction

Hydroxyapatite ($Ca_{10}(PO_4)_6(OH)_2$, hereafter described as HA) has been widely used as a bone replacement material in restorative dental and orthopedic implants, due to its chemical and crystallographic structure similar to that of bone mineral [1–4]. The HA shows excellent biocompatibility with hard tissues, skin and muscle tissues, because it does not exhibit any cytotoxic effects and can be bonded to the bone directly. Thus, HA has become a promising bioactive material for clinical use [5–8]. It is well known, however, that its poor mechanical properties compared to those of human bone are one of the key issues for applications to load-bearing implants [1, 2, 5, 9]. On the other hand, the mechanical properties of some metallic materials, especially Ti and its alloys, are good enough for load-bearing implants, but their biocompatibility is inferior to that of HA [10–13]. A good combination of the bioactivity of HA and the favorable mechanical properties of metals is predicted to be a promising approach to fabricate excellent biomedical materials for load-bearing applications. Once HA is implanted, it is bonded to the bone directly [14], enhancing the fixation in a shorter time and reducing healing time [15–17].

HA coatings have been carried out by various methods such as dip coating, electrophoretic deposition, hot isostatic pressing (HIP), ion-beam sputtering, ion beam dynamic mixing and plasma spraying [18–20]. Among them, plasma spraying has various advantages in chemical composition control, bio-corrosion resistance and process efficiency [3]. Although HA-based composites of Ti or its alloys have been fabricated by plasma spraying, the long term stability of this integration is still questionable. Despite the strong bonding between the Hp coating and bone, it has been recognized that the mechanical stability of the interface is a problem during a surgical operation or after implantation [21, 22].

The bond strength between the HA coating and substrate could be improved by using porous substrate because its porous structure contributes to an increase of contact area with HA. Recently, Oh *et al.* [23] have reported on Young's modulus of porous Ti compacts, which were fabricated by different sintering conditions,

*Author to whom all correspondence should be addressed.

as a function of porosity. They found that Young's modulus of porous Ti compacts is close to human bone at porosities from 32 to 36 vol.%, minimizing damages to tissues adjacent to the implant.

The purpose of this study is to fabricate HA coatings by plasma spraying on porous Ti substrate having similar Young's modulus to human bone, and to investigate the microstructures and bond strengths of HA coatings.

2. Experimental procedures

2.1. Porous Ti substrate

Commercially pure Ti powders with different particle sizes were prepared by the plasma rotating electrode process (PREP) and the gas atomization process in an argon atmosphere. The PREPed powder was produced from pure Ti (grade 2), and the operating conditions of PREP were described elsewhere [23]. The powder was sieved to about 300–500 μm with a mean diameter of 374 μm, and its purity was analyzed to be 99.9%. Gas atomized Ti powder with a high purity of 99.9% (Sumitomo Titanium Corp.) was also sieved in the range of about 45–150 μm with a mean diameter of 65 μm. In this study, the porous Ti substrates were fabricated by hot pressing. Each powder was filled between two ZrO_2 disks in a graphite die of 25 mm in diameter. BN lubricant was sprayed on the graphite punches and inner wall of the die to avoid the reaction between graphite and Ti powder during sintering. In order to attain uniform compaction, the filled powder was pre-pressed at 70 MPa for 0.6 ks before sintering at 1573 K for 7.2 ks for 374 μm powder and at 1373 K for 7.2 ks for 65 μm powder, and then cooled in a furnace in a vacuum of 1×10^{-3} Pa.

Young's modulus of porous Ti substrates was evaluated in the compression test using a rectangular-shaped samples with the size of $9 \times 9 \times 25$ mm^3. Electrical resistance strain gages (base width: 5.2 mm/base length: 16 mm) were mounted on two lateral surfaces to measure longitudinal elastic strain in compression. The test was performed in an elastic range of deformation up to a maximum 1000 N with an applied load of 0.5 N per step. The total porosity of porous Ti substrates was measured by calculating the weight and apparent volume of the specimen. To observe the cross-section of HA coatings, the porous Ti substrates were cut using an electro discharge machine before plasma spraying.

2.2. Plasma spraying of HA

HA powder with a high purity of 99.9 mass% (Sulzer Metco Corp.) was used for plasma spray coating. Disks of porous Ti and bulk Ti with the size of 1 inch in diameter and 5 mm in thickness were prepared as substrates. The bulk Ti disks were cut from the rod of pure Ti (grade 2) used for the PREP. Prior to plasma spraying, the bulk Ti substrates were the blasted with Al_2O_3 grit to roughen the surface, while the porous Ti substrates were coated without blasting treatment. A F4-6 mm (Sulzer Mecto Corp.) was used to realize HA coating. The HA coating was carried out under Ar atmospheric condition. In plasma coating, HA powder was carried by high-purity Ar gas flow to the plasma and sprayed on the substrates by the conditions described in Table I. The bond strength between the HA and substrate was measured using a standard bonding test (ASTM C633-01). The HA coated specimen and jig were bonded using a bonding glue (araldite, Ciba-Geigy Corp), and kept stationary in air for 24 h. Tensile tests were conducted to evaluate the bond strength (Autograph DSS-10T, Shimadzu). The tensile test was carried out at a cross-head speed of 1 mm/min. Five samples were measured to obtain the average bond strength. The surface roughness of the substrates was determined by averaging 10 measurements on each specimen. Scanning electron microscopy (SEM) and X-ray diffraction (XRD) were used to observe surface morphology and determine constituent phase(s) of HA coatings. Element mapping of HA coatings was carried out by SEM-EDX.

TABLE I Plasma spraying parameters employed for preparation of HA coatings

Primary gas (Ar) flow rate (slm)	50
Secondary gas (N_2) flow rate (slm)	6
Current (A)/Voltage (V)	750/58
Spraying distance (mm)	22
Gun transverse speed (cm/min)	2000
Chamber pressure (torr)	200

3. Results and discussion

3.1. Microstructures and properties of porous Ti substrates

Fig. 1 shows SEM micrographs of Ti powders produced by PREP (a) and gas atomization process (b), respectively. The PREPed powder is entirely spherical in shape and possesses a smooth surface. On the other hand, the gas atomized powders have small adhering satellites. Also, the porous Ti compacts sintered at 1573 K using 374 μm powder (c) and at 1373 K using 65 μm powder (d) is shown in Figs 1(c) and (d), respectively. The number of interparticle contacts in the compacts in Fig. 1(c) is significantly less than in Fig. 1(d). These features could be attributed to the surface energy per unit volume, since it depends on the particle diameter. The compact of fine powder possesses high surface energy due to high specific surface area, so that it could be sintered in a short time in spite of a low sintering temperature. The large number of pores in the Ti substrates is considered to be three-dimensionally interconnected.

The properties of bulk Ti and porous Ti substrates used for HA coating were summarized in Table II.

TABLE II Properties of Ti substrates used for HA coating

	Surface roughness (mm)	Total porosity (%)	Young's modulus (GPa)
Non-porous Ti substrate	3.7	0	110
Porous Ti substrate[a]	9.3	32.4	25.0
Porous Ti substrate[b]	33.7	35.6	.1

[a]Substrate sintered with 65 mm powders.
[b]Substrate sintered with 374 mm powders.

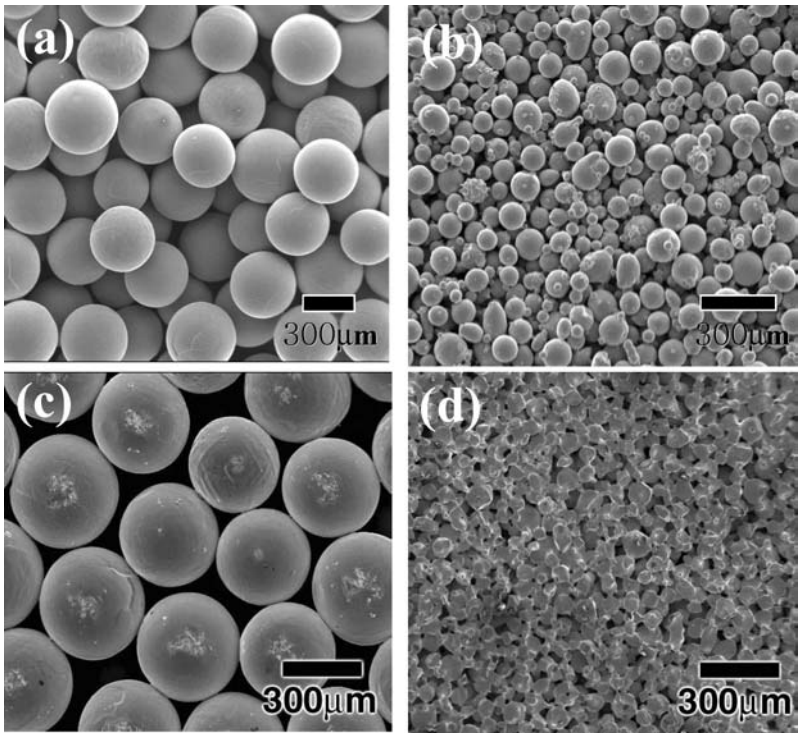

Figure 1 SEM micrographs of starting Ti powders (a, b) and sintered porous Ti compacts (c, d). (a) 300–500 mm (PEEP), (b) 45–150 mm (gas atomization), (c) 1573 K with mean particle 374 mm and (d) 1373 K with mean particle 65 mm.

The surface roughness of porous Ti substrates is higher than that of bulk Ti, and also the roughness of porous Ti substrate is higher in sintering with 374 μm powder than in sintering with 65 μm powder. It is found that the porosities of porous Ti substrates are larger than 30 vol.%. Porous Ti compacts with high porosities of 30–36 vol.% were fabricated by controlling sintering conditions and powder sizes, which meets required properties such as Young's modulus and 0.2% offset yield strength for biomedical applications [23]. It is found that the Young's modulus of porous Ti substrates sintered with smaller particles is higher than that of lager particles. This young's modulus difference is attributed to the surface energy per unit volume, as discussed above. Young's moduli of the present porous Ti substrates with porosities in the range of 32.4 and 35.6 vol.% are almost the same as that of human bone (10–30 GPa) [24–26].

3.2. Microstructures of HA coating

Fig. 2 shows a SEM micrograph and size distribution of HA powder before spraying. The HA powder is nearly spherical in shape with a rough surface (Fig. 2(a)) and has sizes in the range of about 1–77 μm with a mean diameter of 34.1 μm (Fig. 2(b)).

Fig. 3 shows the cross-section views of plasma sprayed HA coatings on the bulk Ti (Fig. 3(a)) and porous Ti substrates (Figs 3(b) and (c)). The surface of porous Ti substrates is roughened depending on the shape of the Ti powder. It is clearly seen that the HA plasma spraying is successfully performed on the three Ti substrates without cracking at the interfaces between the HA and the substrate. The thickness of HA coatings is in the range of 200–250 μm, and there is no significant difference among the three samples. In the porous Ti substrate sintered with 374 μm powder, the melted HA powder penetrates to about 500 μm through pore

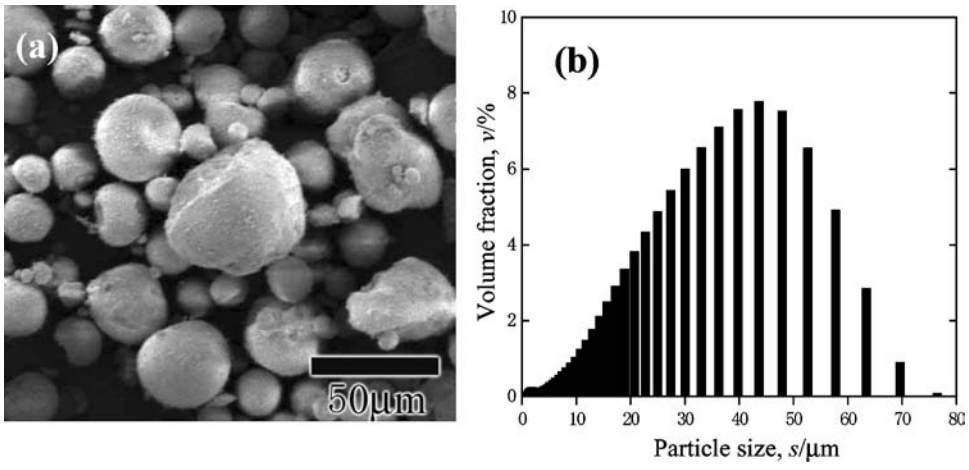

Figure 2 (a) SEM micrograph and (b) size distribution of HA powder used for plasma spraying.

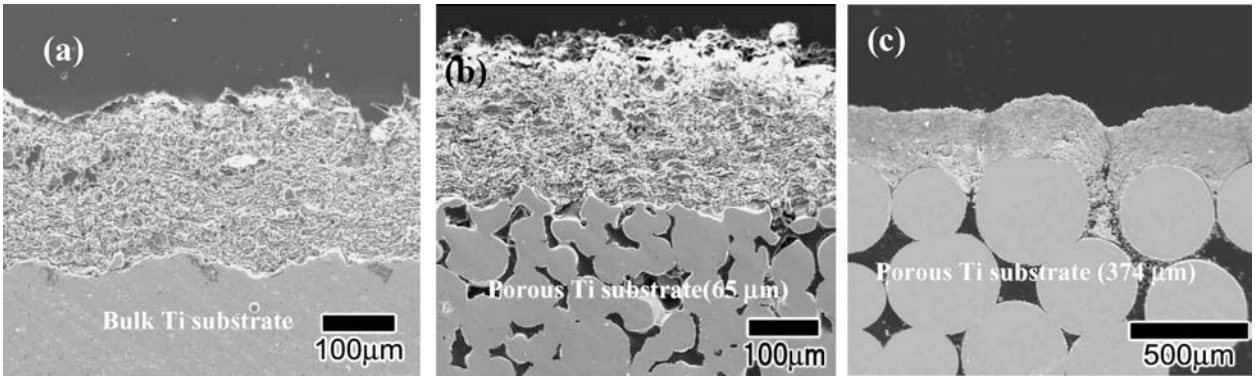

Figure 3 SEM cross-sectional microstructures of HA coatings on (a) bulk Ti, (b) porous Ti substrate sintered with 65 μm powder and (c) porous Ti substrate sintered with 374 μm powder.

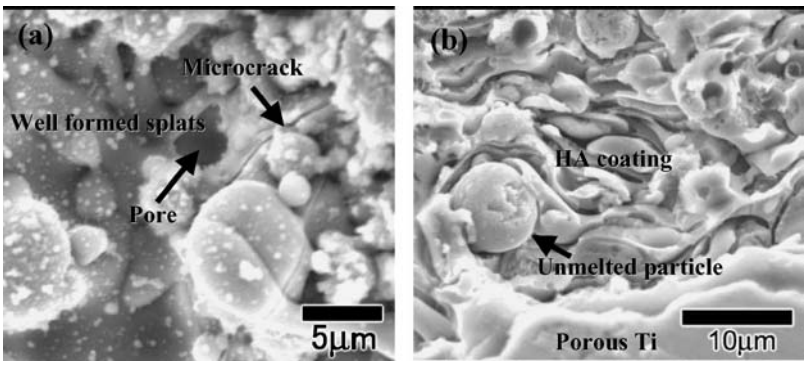

Figure 4 High magnification view (SEM) of a HA coating on porous Ti substrate sintered with 374 μm powder. (a) surface and (b) cross-section.

channels, as shown in Fig. 3(c). From Fig. 3(c), it is considered that the HA penetrating into the porous Ti substrate accelerates a proliferation of body tissue. In other words, when the HA penetrates into the substrate interior, a large amount of bone ingrowth into the pores is expected, which contributes to tight bonding of the bone to the porous Ti.

Fig. 4 shows high magnification views of surface (Fig. 4(a)) and cross-section (Fig. 4(b)) for a plasma-sprayed HA coating on the porous Ti substrate sintered with 374 μm powder. The SEM microstructure in Fig. 4(a) consists of well formed splats from melted particles, micro-cracks and pores, while laminated structures typical in plasma spraying and unmelted particle are observed in the cross-section (Fig. 4(b)). The lamellar structures were denser and good interlamellar contact was evident despite the presence of minute amount of visible voids and interlamellar pores.

Fig. 5 shows the XRD profiles of HA powder (Fig. 5(a)) and as-sprayed HA coating on the porous Ti

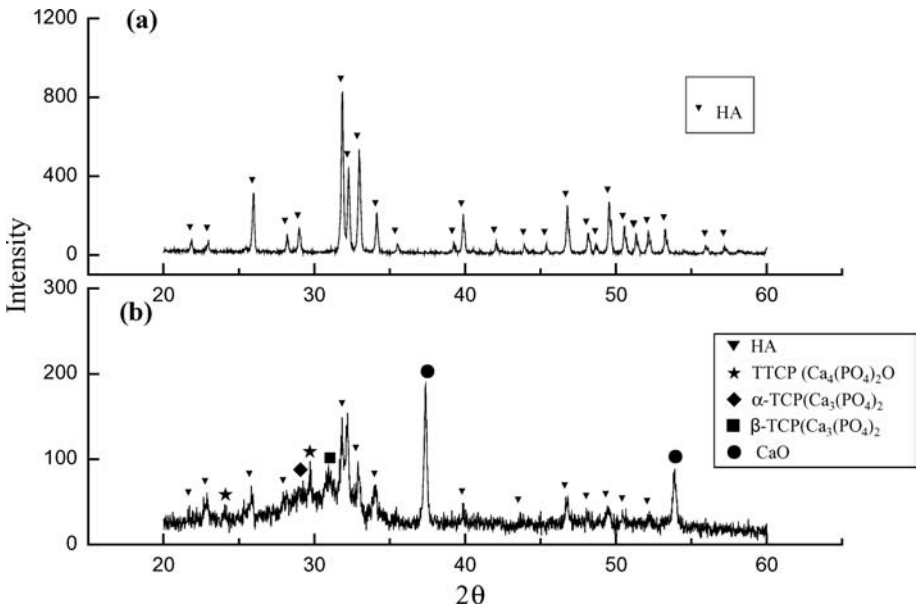

Figure 5 XRD patterns of (a) HA powder and (b) as-sprayed HA coating.

substrate (Fig. 5(b)). As seen clearly, the HA powder used in this study has a highly crystallized structure, while the HA coating exhibits TTCP (Ca_4 $(PO_4)_2O$), α-TCP (Ca_3 $(PO_4)_2$), β-TCP (Ca_3 $(PO_4)_2$) and CaO in addition to HA. Moreover, apatite crystallinity in the as-sprayed HA coating is deteriorated compared with the raw HA powder. When HA is plasma sprayed, (a) HA may be converted into other calcium phosphate phases such as α- or β-tricalcium phosphate, tetracalcium phosphate (TTCP) or calcium oxide (CaO) and (b) crystallinity of HA is lowered due to rapid solidification [4, 27]. Although no apparent amorphous component in the HA coating is observed in this study, it may exist partially in the HA coating due to the rapid quenching of the droplets during spraying [3, 8, 27].

3.3. Bond strength of HA/Ti substrates

The bond strength obtained by a tensile test is shown in Fig. 6. The HA coating shows the highest strength on the porous Ti substrate sintered with 65 μm powder and the lowest on the bulk Ti. Moreover, the HA coating is higher on the porous Ti substrate sintered with 65μm powder than on the porous Ti substrate sintered with 374 μm powder.

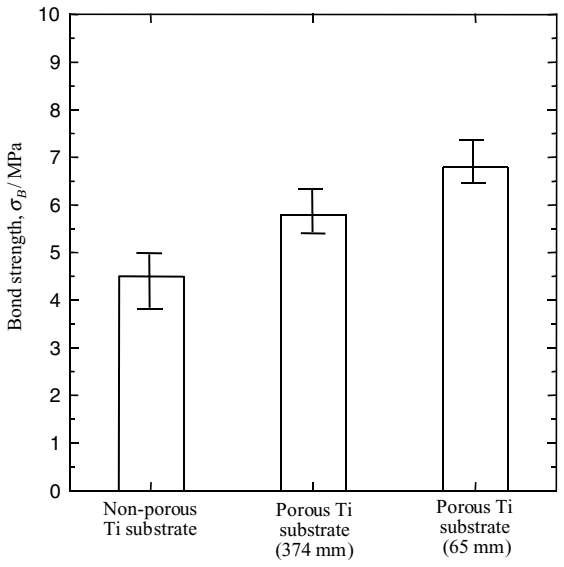

Figure 6 Bond strength of plasma sprayed HA coatings on three different Ti substrates.

SEM micrographs of failure surfaces and schematic illustrations of an interface after the test are shown in Fig. 7. It is obvious that the failure surfaces are different between the bulk Ti (Fig. 7(a)) and porous Ti substrates (Figs 7(b) and (c)). According to ASTM C633-01 specification classifying the failure mode for the plasma-sprayed coating, the adhesive strength of the coating is given if failure is entirely at the coating/substrate interface, and the cohesive strength of the coating is given if failure is only within the coating. Concerning the failure of the coating on the bulk Ti substrate, a SEM micrograph and its illustration are shown in Fig. 7(a) and (d). The sites of adhesive (ad) and cohesive (co) failure of the coating on the porous Ti substrate are indicated respectively by arrows in Fig. 7(c), which are illustrated in Fig. 7(e). Apparently, the failure of HA on the bulk Ti substrate occurred entirely at HA/substrate interface (Fig. 7(d)), i.e. the bond strength corresponds to adhesive strength. The poor adhesive strength of HA coating on the bulk Ti substrate (Fig. 6) is considered to be due to the difference of thermal expansion coefficients (C.T.E) between the Ti substrate (8.4×10^{-6}/K and the HA (13.3×10^{-6}/K coating. Studies on plasma sprayed ceramics coatings on metal substrates have revealed that residual stresses remain at the interface between the coating and the substrate [1, 3, 28]. Consequently, the adhesive strength might be affected by residual stress due to the difference of C.T.E. between the Ti substrate and the HA coating. On the other hand, the surface observation failure of the HA coating on the porous substrates indicates both cohesive and adhesive failures, suggesting that the bond strength is dictated by weak areas within the coating and at the coating/substrate interface (Fig. 7(e)). From both Figs 6 and 7, the combined failure implies that the bonding of the HA coating/porous Ti substrate is higher than

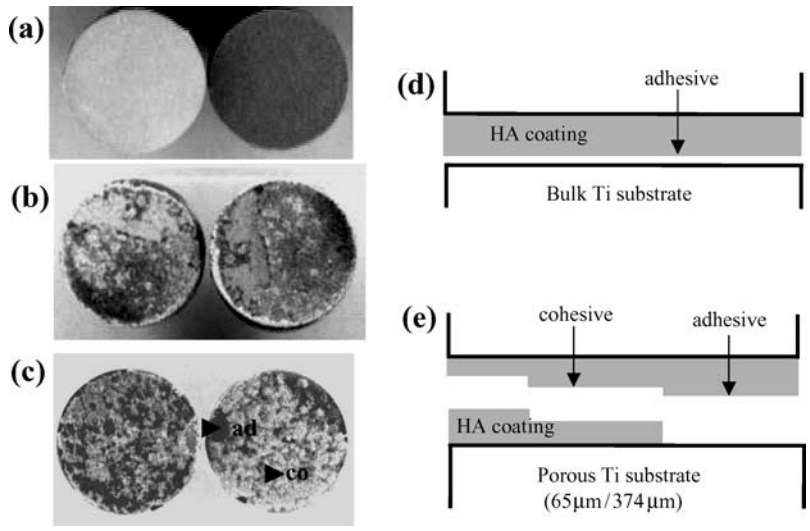

Figure 7 Morphology of failure surfaces of plasma sprayed HA coatings on (a) bulk Ti substrate, (b) porous Ti substrate (374 mm) and (c) porous Ti substrate (65 mm). Schematic illustrations of (d) adhesive failure at HA/bulk Ti substrate and (e) combination of adhesive and cohesive failure at HA/porous Ti substrates (374 and 65 mm).

that of HA/bulk Ti substrate. In contrast, HA coating on a smooth substrate surface is readily spalled. Thus, it is concluded that the bond strength increases with decreasing adhesive failure area, and with increasing cohesive failure area. The cohesive strength might be affected by coating structures such as crystallinity, defects, cracks and lamellar structures. Among the present three Ti substrates, the area fraction of cohesive failure area of HA coating on the porous Ti substrate sintered with 65 μm powder is the highest, as shown in Fig. 7(c). This cohesive failure area of HA coating might be affected by the surface morphology of substrate.

In summary, the bond strength at the interface of the HA/Ti implant is improved by the substitution of porous Ti substrate for bulk Ti. It should be remarked that a good combination of the bioactivity of HA and the favorable mechanical properties of the present porous Ti substrate is indispensable to biomedical applications such as artificial hip joints.

4. Conclusions

Plasma sprayed HA coating on bulk Ti and porous Ti substrates was studied with respect to the microstructure and bond strength. The results obtained are summarized as follows:

(1) HA coating on the bulk Ti and porous Ti substrates is successfully achieved by plasma spraying. The thickness of HA coatings is in the range of 200–250 μm, and no cracks are found at interfaces between HA and Ti substrates.

(2) Bond strength of a HA coating on a porous Ti substrate is higher than that on a bulk Ti substrates. Failure of a HA coating on a bulk Ti substrate occurs entirely at the HA/substrate interface, while the failure of a HA coating on porous Ti substrates occurs at the HA/substrate interface and within the HA coating layer.

Acknowledgments

The present work was partially supported by a Grant-in Aid for Scientific Research on Priority Area (No. 11221202) from the Ministry of Education, Science and Culture, Japan. Also, this work was partially supported by 2002 NRL research program of the Korea Ministry of Science Technology.

References

1. Y. C. YANG and EDWARD CHANG, *Biomaterials* **22** (2000) 1827.
2. C. CHU, J. ZHU, Z. YIN and S. WANG, *Mater. Sci. Eng. A* **A271** (1999) 99.
3. Y. C. TSUI, C. DOYLE and T. W. CLYNE, *Biomaterials* **19** (1998) 2015.
4. S. W. K. KWEH, K. A. KHOR and P. CHEANG, *ibid.* **21** (2000) 1223.
5. X. ZHENG, M. HUANG and C. DING, *ibid.* **21** (2000) 841.
6. G. JIANG and D. SHI, *J. Biomed. Mater. Res.* **43** (1998) 77.
7. J. WENG, X. G. LIU, X. D. LI and X. D. ZHANG, *Biomaterials* **16** (1995) 39.
8. C. F. FENG, K. A. KHOR, E. J. LIU and P. CHEANG, *Scripta Mater.* **42** (2000) 103.
9. B. Y. CHOU and E. CHANG, *Surf. Coat. Techn.* **153** (2002) 84.
10. F. TAKESHITA, Y. AYUKAWA, S. IYMA, K. MURAI and T. SUETSUGU, *J. Biomed. Mater. Res.* **37** (1997) 235.
11. R. NOORT, *J. Mater. Sci.* **22** (1987) 3801.
12. K. HEALY and P. DUCHEYNE, *J. Biomed. Mater. Res.* **36** (1992) 319.
13. M. KHAN, R. WILLIAMS and D. WILLIAMS, *Biomaterials* **20** (1999) 765.
14. R. GEEKINK, K. GROOT and C. KLEIN, *J. Bone Joint Surg.* **70-B** (1988) 17.
15. H. OONISHI, M. YANAMOTO, M. H. ISHIMARU, E. TSUJI and S. KUSHITANI, *J. Bone Joint Surg.* **71-B** (1989) 213.
16. R. LEGEROS, *Clinical Mater.* **14** (1993) 65.
17. J. DALTON and S. COOK, *J. Biomed. Mater. Res.* **29** (1995) 239.
18. T. LI, J. LEE, T. KOBAYASHI and H. AOKI, *J. Mater. Sci.: Mater. Med.* **7** (1996) 355.
19. M. SHIKHANZADEH, *ibid.* **6** (1995) 90.
20. S. BROWN, I. TURNER and H. REITER, *ibid.* **5** (1994) 756.
21. S. COOK, K. THOMAS and J. KAY, *Clin. Orthop.* **265** (1991) 280.
22. J. COLLIER, V. SUPRENANT, M. MAYER, M. WRONA, R. JENSEN and H. SUPERNANT, *J. Arthroplasty* **8** (1993) 389.
23. I.-H. OH, N. NOMURA, N. MASAHASHI and S. HANADA, *Scripta Materialia* **49** (2003) 1197.
24. C. E. WEN, M. MABUCHI, Y. YAMADA, K. SHIMOJIMA, Y. CHINO and T. ASAHINA, *ibid.* **19** (2001) 1147.
25. M. THIEME, K. P. WIETERS, F. BERGNER, D. SCHARNWEBER, H. WORCH, J. NDOP, T. J. KIM and W. GRILL, *Mater. Sci. Forum* **308–311** (1999) 374.
26. M. LONG and H. RACK, *Biomaterials* **19** (1998) 1621.
27. P. CHEANG and K. A. KHOR, *ibid.* **17** (1996) 537.
28. A. EVANS, G. CRUMLEY and R. DEMARAY, *Oxidat. Met.* **20** (1983) 196.

Received 5 March
and accepted 17 November 2004